

# Crosstalk in Multiple-Beam Waveguides

By DETLEF GLOGE

(Manuscript received August 6, 1969)

*Crosstalk limits the number of communication channels which are spatially resolvable at the end of a beam waveguide. The main sources of crosstalk are scattering and distortion by the focusers. A careful study of high quality front surface mirrors led to the results of this paper. The best choice seems to be a periscopic guide made of dielectric mirrors when used with gaussian beams in a particular mode of multiple transmission. We give a closed description for the expected power profile of a gaussian beam that has passed such a guide and an approximate formula for the mutual crosstalk between several such beams.*

## I. INTRODUCTION

Arranging many optical channels spatially resolved in the same waveguide is a simple means for high capacity transmission.<sup>1,2</sup> All channels can be modulated in the same frequency band as long as the crosstalk is kept below a certain threshold. One source of crosstalk is the inevitable scattering from the focusing and directing elements.<sup>3</sup> Diffraction from the ideal beams is negligible.<sup>4</sup> Yet we shall see that diffraction must be considered once the beams are distorted by the focusers.

In all likelihood, these focusers would consist of mirrors because lenses of the size needed are apt to have imperfections within the material. The scattering characteristics of high quality front surface mirrors and lenses of the best quality have been measured recently.<sup>5,6</sup> A comparison shows that the lens scattering was about one order of magnitude larger. Directional changes can easily be accomplished by using periscopic mirror arrangements of the kind shown in Fig. 1.<sup>7</sup> Neglecting aberrations, we consider only the first order focusing effect of these periscopes, which is that of thin convex lenses.

Two methods of multiple channel transmission have been suggested.<sup>2</sup> We discuss these two basic methods with respect to their susceptibility

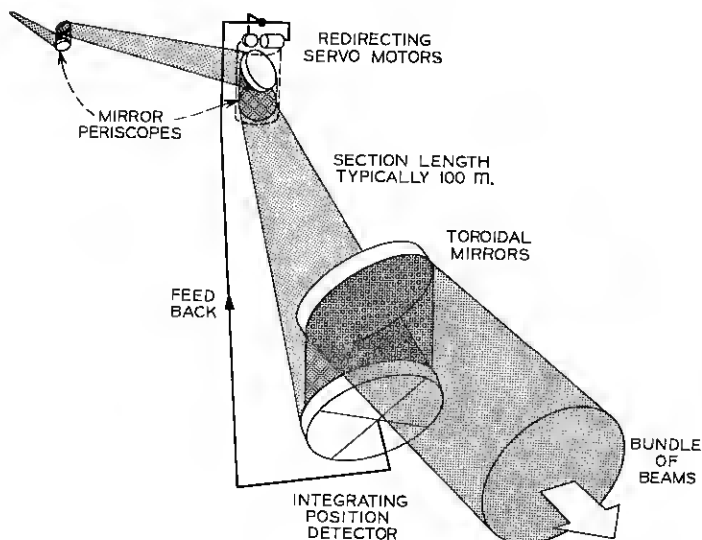


Fig. 1 — Sketch of a periscopic waveguide.

to crosstalk when mirrors of the kind measured in Ref. 5 are used in the waveguide.

## II. MULTIPLE CHANNEL TRANSMISSION

The useful cross section of the beam guide is limited by the size of the periscopic mirrors. Without unreasonable effort, mirrors of good optical quality can be made 20 to 30 cm in diameter at the most. The bundle of beams must clear the mirror edges by a wide margin at all times to guarantee safe operation. This implies that diffraction crosstalk caused by the mirror edges is negligible. Tolerances which would allow for controlled diffraction, as suggested by Ref. 4, seem unreasonably tight. Thus we arrive at a radius  $R$  of about 10 cm for the useful cross section. The spacing  $D$  of the focusers is limited by the terrain and the cost of the straight sections in between. It will most likely be of the order of 100 m. For optimum conditions, the effective focal length of the focusers should be half their spacing, although some deviation can be tolerated in this respect.

Consider the waveguide as a periodic lens system which images an array of transmitters into a similar array of detectors. This is basically what the imaging method (in Fig. 2a) does. Diffraction effects can be minimized if every transmitter radiates a coherent gaussian beam. As

these beams propagate in the guide, their sizes change periodically from the fairly small transmitter spot size to a size close to the cross section of the guide.

This periodic change is avoided by the grouping method sketched in Fig. 2h. The beams arrange in groups and open up to the fundamental mode radius

$$w = \left( \frac{D\lambda}{\pi} \right)^{\frac{1}{2}} \quad (1)$$

before they enter the guide. They keep very close to this radius throughout the transmission. Figure 2b shows the grouping method for two groups containing two beams each. Special collector lenses single out the groups at the end and focus the beams well separated on the detector array. For a better understanding of this detection system, consider the focal length  $f$  of the collector lenses to be short compared to the distance  $D$  between a collector lens and the preceding focuser. In the plane of this focuser, all groups of beams form overlapping patterns. Every collector lens selects the pattern of its group and images it into the detector plane scaled down by a factor  $f/D$ . Consequently, the detector array of every group is confined to a circular area with a radius  $Rf/D$ .

The density of resolvable beams in the system is determined by beam distortion and scattering rather than the spread of the ideal beams. The distortion of the beam profile determines the receiver size required

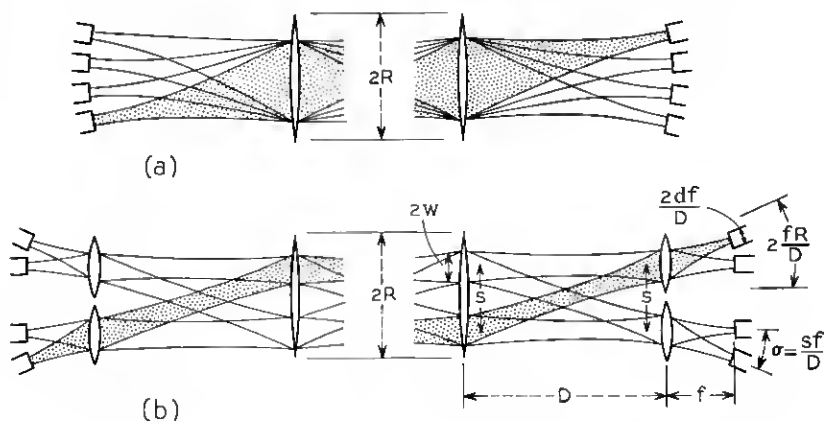


Fig. 2—Schemes for spatially resolved transmission (a) the imaging method (b) the grouping method.

to secure safe reception. One would like to make the detectors as small as possible in order to minimize the scattering collected from adjacent channels. For further reduction of the crosstalk, one has to increase the spacing between the detectors.

Let us assume that the center-to-center spacing is  $s$  for the collector lenses and  $\sigma$  for the detectors in a group. In this case we would have  $\pi R^2/s^2$  groups and  $\pi R^2 f^2/D^2 \sigma^2$  beams per group if the guide were perfectly confocal. If we allow a slight tolerance for the spacing of the focusers, Ref. 2 shows that the groups belonging to off-center collector lenses cannot be completely filled. For this reason the total number of channels is only half the theoretical maximum, namely

$$N = \frac{1}{2} \frac{\pi^2 R^4 f^2}{s^2 \sigma^2 D^2}. \quad (2)$$

Rather than considering the detector plane, let us look at the distribution every group has at the focuser preceding a collector lens. This way our results become independent of the focal length  $f$  of the collector lenses and a function of the beam waveguide only. In the plane of the last focuser the beam spacing is  $D\sigma/f$ . As the beams have the same width there as at the collector lenses, it seems reasonable to set

$$s = D\sigma/f. \quad (3)$$

Inserting this into equation (2) yields

$$N = \frac{\pi^2}{2} \left( \frac{R}{s} \right)^4. \quad (4)$$

In the following let us assume that the detectors are simple quantum counters, have a circular area, and have a radius  $d f/D$ . Transforming this back to the last focuser, we find a circular area of radius  $d$  susceptible to crosstalk around every beam. In Section II we evaluate scattering and distortion of a single beam in the plane of the last focuser for the case of a waveguide of  $n$  mirror periscopes. Since we use direct detection, we may neglect phase front distortion. The case of heterodyne reception is briefly discussed in the appendix. The results are very similar to those of the direct detectors.

## II. DISTORTION AND SCATTERING

Both distortion and scattering are a consequence of irregularities on the mirror surfaces. The distortion originates from smooth imperfections extending over areas comparable to the beam cross section

while scattering is caused by a surface roughness correlated over distances much smaller than the beam diameter. Both irregularities are part of a statistical function  $\delta(x, y)$  which describes the deviation from the ideal surface. Taking a meaningful average over an ensemble of test surfaces leads to the structure function

$$\Delta(\rho) = \langle [\delta(x, y) - \delta(x - \rho \cos \alpha, y - \rho \sin \alpha)]^2 \rangle_{av} \quad (5)$$

where  $\rho$  and  $\alpha$  belong to a polar coordinate system which has the point  $(x, y)$  as its origin. Writing  $\Delta$  as a function of  $\rho$  only implies the assumption that  $\delta$  is stationary and isotropic, which seems justified for the statistical properties involved.<sup>5</sup>

A light wave of wavelength  $\lambda$  reflected off the imperfect surface suffers a phase front distortion

$$\varphi(x, y) = \frac{4\pi}{\lambda} \delta(x, y). \quad (6)$$

We neglect reflection loss which we assume to be uniform over the surface. For gaussian statistics<sup>4</sup>

$$\langle \exp i[\varphi(x, y) - \varphi(x - \rho \cos \alpha, y - \rho \sin \alpha)] \rangle_{av} = \exp \left[ -\frac{8\pi^2}{\lambda^2} \Delta(\rho) \right]. \quad (7)$$

This equality will be used to calculate the power distribution  $p_1(r)$  at a distance  $D$  from the reflecting surface. Assume that the reflected beam is circular, symmetric, and would have a power profile  $p_0(r)$  at a distance  $D$  if the reflection were ideal. Then, from Ref. 8, one obtains

$$g_1(\rho) = g_0(\rho) \exp \left[ -\frac{8\pi^2}{\lambda^2} \Delta(\rho) \right] \quad (8)$$

where  $g_1(\rho)$  and  $g_0(\rho)$  are the Hankel transforms of  $p_1(r)$  and  $p_0(r)$ , respectively. This Hankel transformation is defined by

$$g_1(\rho) = 2\pi \int_0^\infty p_1(r) J_0(2\pi \rho r / D\lambda) r \, dr \quad (9)$$

or

$$p_1(r) = \frac{2\pi}{D^2 \lambda^2} \int_0^\infty g_1(\rho) J_0(2\pi \rho r / D\lambda) \rho \, d\rho \quad (10)$$

where  $J_0$  is the Bessel function of zero order. The quantity  $p_1(r)$  has to be understood as an average over an ensemble of equivalent surfaces.

For an accurate confocal spacing of the periscopes, a beam and its

distortion in the guide reproduces itself at every second periscope. These periscopes only contribute to the phase front distortion in the detector plane, while all odd ones deteriorate the power profile as well. We have  $n$  periscopes with  $2n$  surfaces, half of them contributing to the profile distortion. Since the imperfections of all surfaces are uncorrelated, we may write

$$g_n(\rho) = g_0(\rho) \exp \left[ -\frac{8\pi^2}{\lambda^2} n \Delta(\rho) \right] \quad (11)$$

for the detector plane.

In a guide with thousands of focusers, accurate confocal spacing requires tight tolerances for the focal lengths and spacings. In a practical guide, the focusers will be kept only nearly confocal and, in general, will not be at positions at which previous distortions are reproduced. If all positions are equally probable along the guide, equation (11) can be adapted in the following way<sup>8</sup>

$$g(\rho) = g_0(\rho) \exp \left[ -\frac{8\pi^2}{\lambda^2} \frac{2n}{\pi} \int_0^\pi \Delta(\rho \sin \xi) d\xi \right]. \quad (12)$$

Notice that for  $\xi = 0$  or  $\pi$ , we have  $\Delta(0) = 0$  and no change of the power distribution, while for  $\xi = \pi/2$  the profile distortion is a maximum.

A fairly reliable functional approximation for  $\Delta$  in the range  $\rho = 0.01$  to 1 mm was derived from scattering measurements around a test beam.<sup>5</sup> The scattering is an effect of the mirror surface roughness averaged over the area covered by the test beam. This average is equivalent to an average over an ensemble of test surfaces. As a consequence, the variance of the scattered power is small, that is, the scattered power actually measured is very close to the average power. The measurements were practically the same for all test surfaces.

This is not true for the processes involved in beam distortion. In this case, the  $\delta$ -components participating are correlated over areas comparable to the test beam, no averaging is accomplished by the measurement, and the result can be grossly different from one surface to the next. It is this difference between scattering and distortion which makes scattering measurements feasible but distortion measurements tedious and expensive. Distortion is not sufficiently described by an average power profile; instead one needs to know the complete probability distribution of the power at every point in the beam cross section. In this situation some grossly simplifying assumptions are necessary to tackle the distortion problem with the scant experimental evidence available.

We derived the functional approximation

$$\Delta(\rho) = E\rho \quad \text{for } \rho = 0.01 \cdots 1 \text{ mm} \quad (13)$$

with

$$E = 2.4 \times 10^{-9} \mu \quad (14)$$

from measurements.<sup>5</sup> This approximation is plotted in Fig. 3. For larger  $\rho$  we have only one reference point: the quality factor of the mirror, given in fractions of the green wavelength, which specifies  $\delta$ -components correlated over areas comparable to the polishing tool. This will be typically several centimeters. We know  $\Delta$  decreases for smaller  $\rho$  and merges into the linear function (13) at  $\rho = 1$  mm. As a convenient approximation, let us assume that  $\Delta$  is linear everywhere. This function would correspond to about  $\lambda_{\text{green}}/50$  at several cm.

Whether equation (13) is a good approximation for  $\rho < 0.01$  mm we do not know, but this is of little interest, since components at these small  $\delta$  generate scattering which does not reach the next focuser, but is absorbed by the guide wall.

A gaussian beam of unit power has the profile

$$p_0(r) = \frac{2}{\pi w^2} \exp(-2r^2/w^2). \quad (15)$$

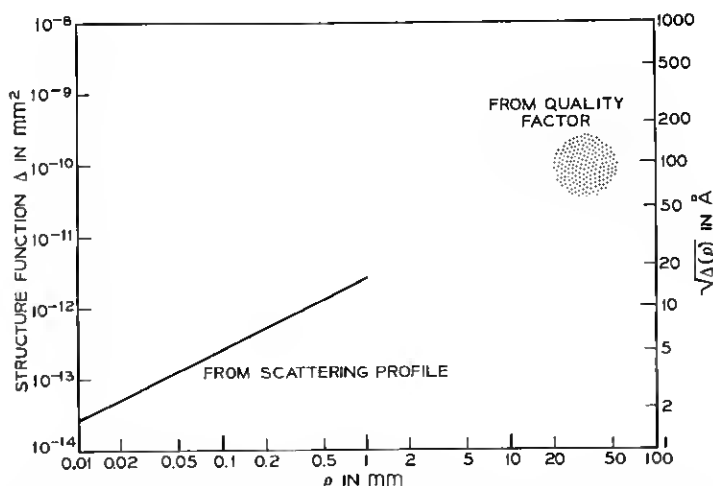


Fig. 3—The linear structure function  $\Delta(\rho)$  calculated from scattering profile and quality tests.

Its Hankel transform is

$$g_0(\rho) = \exp(-\pi^2 w^2 \rho^2 / 2D^2 \lambda^2). \quad (16)$$

Using equations (10), (12), (13), and (16), we find the following average power distribution at the detector

$$p(r) = \frac{2}{\pi w^2} \int_0^\infty \exp\left(-\frac{u^2 + au}{2}\right) J_0\left(\frac{2ur}{w}\right) u \, du \quad (17)$$

where

$$u = \frac{\pi w}{D\lambda} \rho \quad \text{and} \quad a = 64 \frac{wED}{\lambda w}. \quad (18)$$

The average power falling outside a circular area of radius  $z$  is

$$P(z) = 2\pi \int_z^\infty p(r)r \, dr. \quad (19)$$

Using the identity

$$J_1(z)z = \int_0^z J_0(v)v \, dv, \quad (20)$$

we arrive at

$$P(z) = 1 - \frac{2z}{w} \int_0^\infty \exp\left(-\frac{u^2 + au}{2}\right) J_1\left(\frac{2uz}{w}\right) du. \quad (21)$$

The result of the machine evaluation of equation (21) is plotted in Fig. 4. For  $a = 0$  the beam is undistorted and  $P(z)$  is gaussian. Yet  $P(z)$  has a tail decreasing with  $1/z$  for finite  $a$ .

In the course of our calculation we want to know the radius  $z$  outside of which a given power  $P$  can be found for a certain parameter  $a$ . For this purpose the function  $z(P, a)$  is plotted in Fig. 5. It can be approximated by the expression

$$z = \left[ w^2 \ln \frac{1}{P^2} + \left( \frac{16EnD}{\lambda} \right)^2 \left( \frac{1}{P^2} - 1 \right) \right]^{\frac{1}{2}} \quad (22)$$

where equation (18) was inserted for  $a$ .

The first part of equation (22) is an inverse gaussian and depicts the coherent beam, while the second part accounts for the incoherent portion. Equation (22) can be used, for example, to calculate the detector radius required at the end of a periscopic guide. In this case one will probably allow the second term in equation (22) to be about



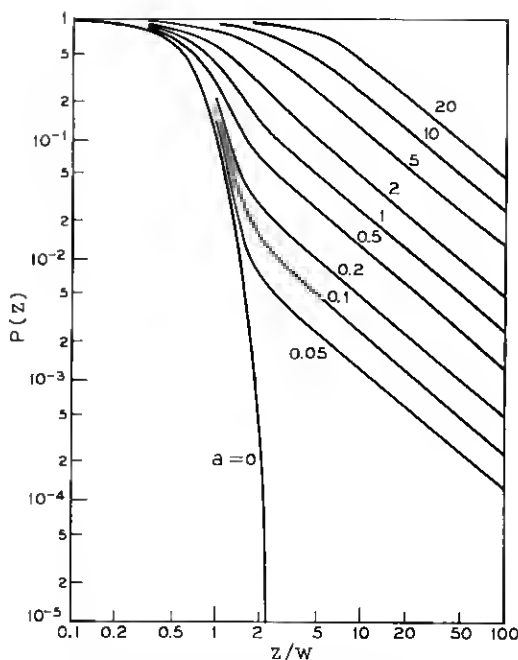


Fig. 4 — The power fraction  $P$  expected outside the circular area with the normalized radius  $z/w$  for various distortion coefficients  $\alpha$ .

equal to the first. This would mean that the beam deterioration becomes just noticeable, but not yet dominating, at the end.

We shall find another application for equation (22) in the course of calculating the scattering crosstalk. In this case we require  $P$  to be so small that the second term in equation (22) exceeds the first even for moderate distortions, and equation (22) can be approximated by

$$z \cong \frac{16EnD}{\lambda P}. \quad (23)$$

Notice that the only guide dimension that enters into this formula is the total transmission distance

$$L = nD \quad (24)$$

from one repeater to the next. Equation (22) leads to an estimate for the detector sizes required and with this information and the help of equation (23) we can evaluate the scattering crosstalk.

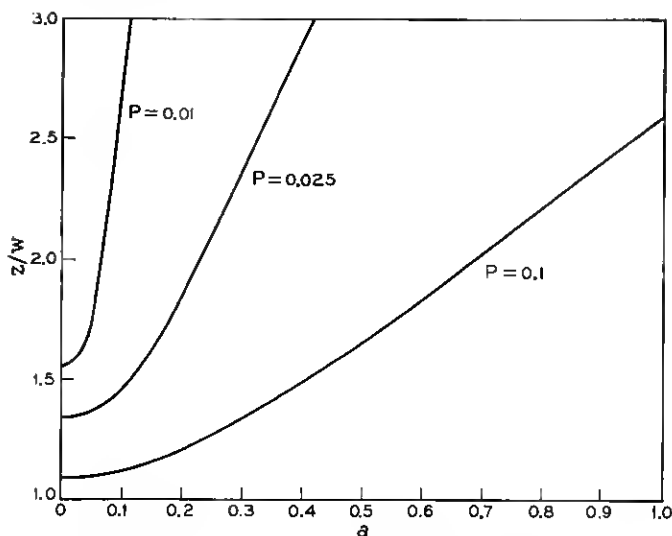


Fig. 5 — The functional relation  $z(a)$  with  $P$  as a parameter.

#### IV. BEAM SPREAD AND CROSSTALK

The interchannel crosstalk at the end of the multiple beam guide is a function of the detector size. In order to minimize the amount of light collected from other channels, the detectors should not be larger than is absolutely necessary for signal detection. A few percent of the signal power could even be sacrificed. The signal fraction to be detected will depend on the signal levels available and on the noise sources involved, but it is probably safe to assume that, on the average, 75 percent of the total signal power will be sufficient. Thus we obtain from equations (22) and (24) for the detector radius

$$d = \left[ w^2 \ln 2 + 15 \left( 16 \frac{LE}{\lambda} \right)^2 \right]^{\frac{1}{2}}. \quad (25)$$

In a more general sense, we may interpret  $d$  as the average radius of a distorted beam at the end of a guide of length  $L$ . In equation (25),  $w$  is the radius of the ideal gaussian beam which may vary considerably along the guide as, for example, in the case of the imaging method. For the grouping method,  $w$  is constant and given by equation (1).

To compare both methods, let us consider a practical example of a waveguide with 100 m section length operating at a wavelength of  $1 \mu\text{m}$  over a distance of 50 km. If we use the grouping method, we find

$w = 5.65$  mm from equations (1) and (25) yields a beam radius of 8.8 mm. In the case of the imaging method,  $w$  varies about 5.65 mm from lens to lens, being much smaller than 5.65 mm at the detectors. Yet at the end of a 50 km path, the average radius of the distorted beams will not be smaller than 7.5 mm because of the second part of equation (25). This is only slightly less than the radius of the grouped beams. It is obvious from Fig. 2 that under these circumstances the imaging method loses its advantage. Actually, in this case, the imaging method can only accommodate the beams contained in one group of the grouping method. Therefore, in the following we consider only the grouping method.

For the calculation of the scattering crosstalk we restrict ourselves to paraxial beams. Any two beams of this kind are equivalent in the sense that the amount of light scattered from a beam 1 into another beam 2 is equal to the amount scattered from 2 into 1. In the same way, the scattering from one beam into all others is what the beam receives from all others. This is exactly the crosstalk we want to calculate. Thus, in order to consider the worst situation, let us select the center beam and calculate what it scatters into all extraneous receivers. To do this we have to integrate the scattered power falling into the detector plane, excepting the center detector and the blind area between all detectors. We remember that the detectors have a radius  $d$  and are spaced by a distance  $s$  center to center. We obtain a reasonable and conservative approximation if we collect all the scattering outside a circle with radius  $s/2$ , which is  $P(s/2)$  from equation (21), and multiply this by a density factor  $\pi d^2/s^2$ . Consequently, the crosstalk which the center beam inflicts upon, and receives from, all other beams is

$$C = \frac{\pi d^2}{s^2} P(s/2). \quad (26)$$

For all practical cases the tolerable  $C$  is so small that we may use the approximation (23) for  $P$ . Inserting equations (1), (24), and (25) into equation (26) we obtain

$$C = 32 \frac{LDE}{s^3} \ln 2 + 30\pi \left( \frac{16LE}{\lambda s} \right)^3. \quad (27)$$

Figure 6 shows the signal to crosstalk ratio  $1/C$  plotted in decibel versus the spacing  $s$  for the previous example, that is,  $D = 100$  m and  $\lambda = 1$   $\mu$ m. Also shown is the guide capacity  $N$  to be achieved by the grouping method in a guide of 10 cm radius. The transmission distance  $L$  between repeaters is the parameter. For reasons explained previously,

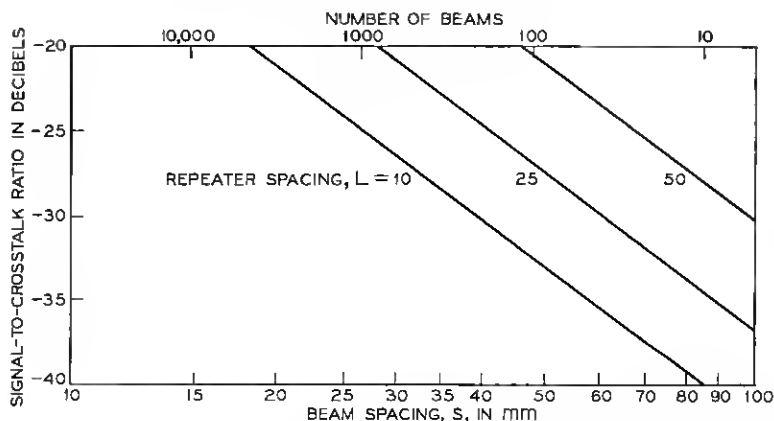


Fig. 6—Crosstalk versus the beam density and the capacity for various repeater spacings ( $\lambda = 1 \mu\text{m}$ ,  $D = 100 \text{ m}$ , and  $R = 100 \text{ mm}$ ).

the capacity achieved by the imaging method is less, for practical systems only about  $N^{1/2}$ . Figure 7 shows the useful guide radius required for a certain capacity at various repeater spacings if a crosstalk level of 23 dB is tolerable. Both Figs. 6 and 7 exhibit a system with  $N = 100$ ,  $L = 50 \text{ km}$ ,  $R = 10 \text{ cm}$ ,  $D = 100 \text{ m}$ ,  $\lambda = 1 \mu\text{m}$ , and  $C = 23 \text{ dB}$  as feasible but also (more or less) as a practical limit.

The grouping method uses collector lenses in front of the detectors. Diffraction at these lenses must not cause excessive crosstalk even if the beams are badly distorted. For this reason the apertures have to be fairly large. If the available space is fully used, the lenses touch one another and are arranged as in a fly's eye lens. The lenses should be so large that the power at the lens edges is mainly incoherent and not part of the coherent, though distorted, beam. In this case, diffraction does not substantially increase the total power outside the signal beams. This requirement sets a lower limit to the beam spacing  $s$  which is simultaneously the diameter of the collector lenses. How far this limit is approached by the system depicted in Figs. 6 and 7 is a difficult question to answer.

A qualitative approach is tried in Fig. 8 where the previous results are also summarized. Figure 8 shows the power expected outside a given aperture after a beam has passed a length  $L$  of periscopic waveguide. The beam is supposed to start with a fundamental mode radius  $w = 5.65 \text{ mm}$  in a guide with 100-m section length. Also shown is the power  $P(s/2)$  falling outside a collector lens of radius  $s/2$  where  $s$  is

chosen with the help of equation (27) to guarantee a crosstalk level of  $C$  dB. Thus, once we have decided on the crosstalk level and the transmission distance, we find the radius of the collector lens and the power falling outside this lens from Fig. 8. For  $L = 50$  km and  $C = 23$  dB, this power seems to be composed mainly of scattered light so that diffraction should contribute little to the overall crosstalk.

Several discrepancies become apparent when the results of this paper are compared to previous publications. The power  $P$  falling outside a circle with a radius  $z$  after only one reflection is obtained if we replace equation (12) by equation (11) and set  $n = 1$  in the derivation of equation (23). In the case of a linear structure function, equations (11) and (12) differ by a factor  $\pi/4$ , and therefore

$$P = 4\pi \frac{ED}{\lambda z}. \quad (28)$$

The same physical problem was approached on a different course in Ref. 5 and is expressed in equation (16) there. That result differs from our equation (28) by a factor of four. The reason is a factor of four erroneously introduced in equation (13) of that publication.

In Ref. 3 the crosstalk of one beam into one other beam was measured. This quantity can be calculated on the basis of this paper. The

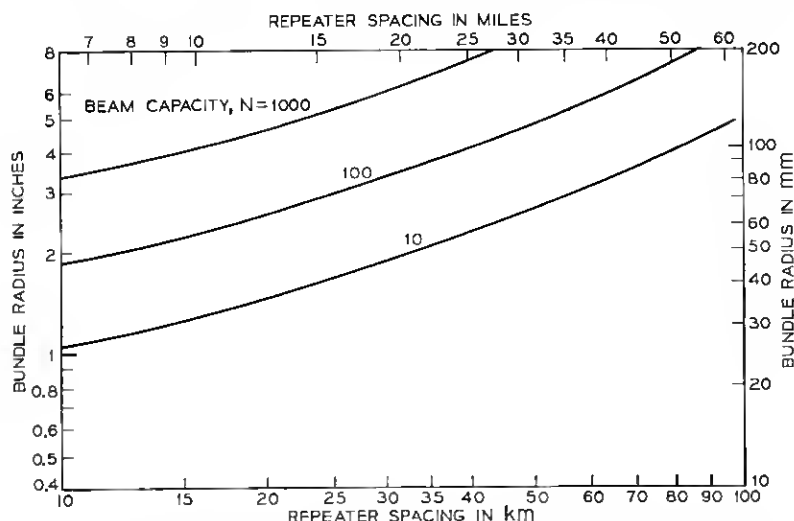


Fig. 7—The beam bundle radius versus the repeater spacing for a given capacity  $N$  (signal/crosstalk = 23 dB,  $\lambda = 1 \mu\text{m}$ , and  $D = 100$  m).

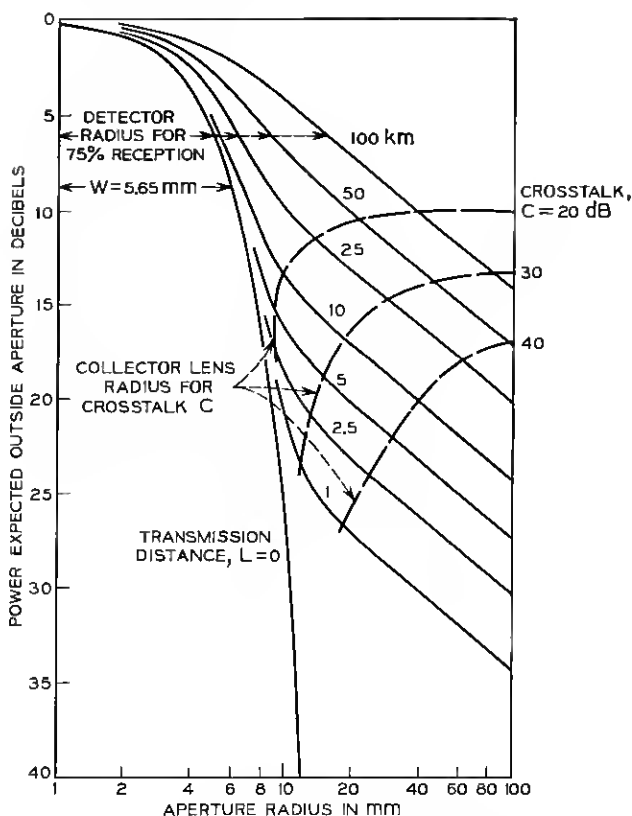


Fig. 8—The power fraction expected outside the collector lens aperture for various repeater spacings and crosstalk levels (section length = 100 m; wavelength =  $1 \mu\text{m}$ ).

power density at a distance  $z$  from a scattering beam is

$$q = -\frac{1}{2\pi z} \frac{dP}{dz} \quad (29)$$

with  $P(z)$  from equation (23). A small aperture of radius  $d$  displaced by a distance  $s$  from the beam center collects approximately

$$c = \pi d^2 q(s) \quad (30)$$

with  $q$  from equation (29). This is the crosstalk in the second beam. With equations (23), (29), and (30) we obtain

$$c = \frac{8d^2 EL}{\lambda s^3}. \quad (31)$$

The specific dimensions in the experimental arrangement of Ref. 3 were  $s = 5$  mm,  $d = 2.5$  mm, and  $\lambda = 0.63$   $\mu$ m. The transmission distance was equivalent to 8.5 km of a periscopic guide. By inserting these data into equation (31) we obtain a crosstalk level of 19 dB. The measured level was 30 dB. Moreover, equation (31) suggests that the crosstalk decreases with the third power of the beam spacing. In Ref. 3, on the other hand, a decrease with the fourth power of the beam spacing was measured. The reason for the discrepancy is still under investigation. The comparison seems to indicate that the data used here are on the conservative side.

Finally let us compare our results to the diffractive crosstalk which ideal gaussian beams experience along a wave guide. Reference 4 considers this situation giving the following results. A guide of 10,000 focusers, 100 m apart and 5 cm in diameter, could accommodate 16 beams with only 60 dB crosstalk. According to our findings, scattering in this arrangement causes 50 dB crosstalk in one 100 m section. This underlines the severe limit which scattering and distortion set to multi-beam transmission. Improving the optical surfaces would be a worthwhile undertaking.

## V. CONCLUSIONS

Scattering and distortion of the beams in a beam waveguide are caused by surface irregularities of the focusers. There is experimental evidence that these irregularities can be described, as a first approximation, by a linear structure function. Based on these findings we predict a beam distortion and an incoherent background radiation which both increase with the transmission distance  $L$ . The distortion makes it impossible to use a simple transmission method which images an array of transmitters into the detector plane. The method which seems more practical arranges the beams in groups and transmits them with unvariable width.

The incoherent background of scattered light around every beam fades off with the third power of the distance from the beam. This causes a crosstalk inversely proportional to the third power of the beam spacing. The beam density is limited by the crosstalk tolerable after 50 km. If we set this level at 23 dB, allow a beam bundle 20 cm in diameter, and operate at a wavelength of 1  $\mu$ m, we could accommodate about 100 beams. This is based on the assumption that periscopic focusers are used which are made of high quality front surface mirrors. A critical comparison with previous publications suggests that our results are conservative, if not pessimistic.

## APPENDIX

*Heterodyne Detection*

One might consider heterodyne detection as a way to reduce the scattering received in every channel. Local oscillator beams could be brought in line with the signal beams, utilizing beam splitters. The local oscillator beams would discriminate to a certain extent against the incoherent background of scattered light from other channels. To compare this with the quantum counters discussed in the text, let us assume that the scattered background light is uniform in the vicinity of the local oscillator beam. For this case Siegman has calculated the IF-photocurrent noise of heterodyne reception.<sup>9</sup> He found that the "integrated effective detector area" of the heterodyne detector is equal to  $\lambda^2$ .

We now calculate the "effective detector area" for our quantum detectors. Every detector has an area

$$A_1 = \frac{\pi d^2 f^2}{D^2} \quad (32)$$

and is preceded by an aperture with the area

$$A_2 = \pi s^2. \quad (33)$$

The distance between aperture and detector is  $f$ . From Ref. 10 we find the "effective detector area" for this arrangement to be

$$\frac{A_1 A_2}{f^2} = \frac{\pi^2 s^2 d^2}{D^2}. \quad (34)$$

Inserting equation (1) we obtain

$$\frac{A_1 A_2}{f^2} = \frac{s^2 d^2}{w^4} \lambda^2. \quad (35)$$

If we had  $sd = w^2$ , the quantum counter would discriminate as well against scattering as the heterodyne detectors.

In the case of distorted signal beams, however, both schemes cannot recover the full signal power. What is important in this case is the ratio of signal to background light collected in the respective cases. For this reason, the quantum counter can be equivalent to the heterodyne detector even if  $s$  and  $d$  are slightly larger than  $w$ . However, for reasons explained in Section IV,  $s$  will be considerably larger than  $w$  to avoid diffractive crosstalk. The heterodyne receiver therefore surpasses the quantum counter. On the other hand, the complexity of the former probably makes up for this advantage.



## REFERENCES

1. Rosenthal, J. E., "Modulation of Coherent Light," *Bull. Amer. Phys. Soc.* II, 6, No. 1 (February 1, 1961), p. 68.
2. Gloge, D., and Weiner, D., "The Capacity of Multiple Beam Waveguides and Optical Delay Lines," *B.S.T.J.*, 47, No. 10 (December 1968), pp. 2095-2109.
3. Gloge, D., and Steier, W. H., "Experimental Simulation of a Multiple Beam Optical Waveguide," *B.S.T.J.*, 48, No. 5 (May 1969), pp. 1445-1457.
4. Goubau, G., and Schwering, F. K., "Diffractional Crosstalk in Beam Waveguides for Multibeam Transmission," *Proc. IEEE*, 56, No. 9 (September 1968), pp. 1632-1634.
5. Gloge, D., Chinnock, E. L., and Earl, H. E., "Scattering from Dielectric Mirrors," *B.S.T.J.*, 48, No. 3 (March 1969), pp. 511-526.
6. Hostetter, G. R., Patz, D. L., Hill, H. A., and Zanoni, C. A., "Measurement of Scattered Light from Mirrors and Lenses," *Appl. Opt.*, 7, No. 7 (July 1968), pp. 1383-1385.
7. Gloge, D., "Experiments with an Underground Lens Waveguide," *B.S.T.J.*, 46, No. 4 (April 1967), pp. 721-735.
8. Gloge, D., unpublished work.
9. Siegman, A. E., "The Antenna Properties of Optical Heterodyne Receivers," *Proc. IEEE*, 54, No. 10 (October 1966), pp. 1350-1356.
10. Kogelnik, H., and Yariv, A., "Considerations of Noise and Schemes for its Reduction in Laser Amplifiers," *Proc. IEEE*, 52, No. 2 (February 1964), pp. 165-172.

